

Supernova Ia: a Converging Delayed Detonation Wave

N.V.Dunina-Barkovskaya, V.S.Imshennik*, S.I.Blinnikov

Institute for Theoretical and Experimental Physics, Moscow, Russia

Max-Planck-Institut für Astrophysik, Garching, Germany

Submitted to Astronomy Letters on 25.12.2000

Abstract

A model of a carbon-oxygen (C–O) presupernova core with an initial mass $1.33M_{\odot}$, an initial carbon mass fraction $X_{\text{C}}^{(0)} = 0.27$, and with an average mass growth-rate $5 \cdot 10^{-7}M_{\odot} \text{ yr}^{-1}$ due to accretion in a binary system was evolved from initial density $\rho_{\text{c}} = 10^9 \text{ g cm}^{-3}$, and temperature $T_{\text{c}} = 2.05 \cdot 10^8 \text{ K}$ through convective core formation and its subsequent expansion to the carbon runaway at the center. The only thermonuclear reaction contained in the equations of evolution and runaway was the carbon burning reaction $^{12}\text{C}+^{12}\text{C}$ with an energy release corresponding to the full transition of carbon and oxygen (with the same rate as carbon) into ^{56}Ni . As a parameter we take α_{c} — a ratio of a mixing length to the size of the convective zone. In spite of the crude assumptions, we obtained a pattern of the runaway acceptable for the supernova theory with the strong dependence of its duration on α_{c} . In the variants with large enough values of $\alpha_{\text{c}} = 4.0 \cdot 10^{-3}$ and $3.0 \cdot 10^{-3}$ the fuel combustion occurred from the very beginning as a prompt detonation. In the range of $2.0 \cdot 10^{-3} \geq \alpha_{\text{c}} \geq 3.0 \cdot 10^{-4}$ the burning started as a deflagration with excitation of stellar pulsations with growing amplitude. Eventually, the detonation set in, which was activated near the surface layers of the presupernova (with $m \simeq 1.33M_{\odot}$) and penetrated into the star down to the deflagration front. Excitation of model pulsations and formation of a detona-

tion front are described in detail for the variant with $\alpha_{\text{c}} = 1.0 \cdot 10^{-3}$.

Keywords: supernovae and supernova remnants; plasma astrophysics; hydrodynamics and shock waves; detonation and deflagration.

Introduction

Evolution of a degenerate C–O stellar core with a mass close to the Chandrasekhar limit ($1.43M_{\odot}$ for a carbon white dwarf, see Bisnovaty-Kogan, 1989) leads to the development of thermal instability and to the explosion. The critical density $\rho_{\text{c cr}}$ for the beginning of the explosion may vary from $\sim 2 \cdot 10^9$ to $\sim 10^{10} \text{ g cm}^{-3}$. It increases with reduction of \dot{M} — the core mass growth-rate which for a single asymptotic giant branch (AGB) star is defined by the Paczyński — Uus relation (Paczyński, 1970)

$$\dot{M} = 6 \cdot 10^{-7} (M/M_{\odot} - 0.5) M_{\odot} \text{ yr}^{-1}, \quad (1)$$

and can take values from 10^{-8} to $5 \cdot 10^{-7}M_{\odot} \text{ yr}^{-1}$ in an accreting white dwarf (Iben, 1982; Hachisu et al., 1996). In the present paper we assume $\dot{M} = 5 \cdot 10^{-7}M_{\odot} \text{ yr}^{-1}$ which can be appropriate both for a single AGB-star and for a component of a binary system.

The explosion calculations, some of which accounted for convection, were carried by various authors (Arnett, 1969; Ivanova et al., 1974; Nomoto et al., 1976; see also the review by Niemeyer and Woosley (1997)). Ivanova et al.(1974) found that

*email: imshennik@vxitep.itep.ru

carbon was burning in the deflagration regime with excitation of pulsations, but convection at the supernova stage was not considered, and the initial temperature profile was obtained not from evolutionary calculations, but from an estimate of a convection contribution.

Woosley (1997) has carried out a series of one-dimensional explosion calculations for accreting white dwarfs (unfortunately, in this work the accretion rates are not specified) with critical central densities from $2 \cdot 10^9$ to $8.2 \cdot 10^9 \text{ g cm}^{-3}$ and with nuclear reactions for 442 isotopes, but he considered only the adiabatic convection at the presupernova stage, while at the beginning of the thermal runaway (when $T_c = 7 \cdot 10^8 \text{ K}$) he turned off the convection artificially (because further maintenance of the adiabatic temperature gradient in his model led to the prompt detonation), and defined the burning front propagation velocity according to Woosley and Timmes (1992) with a provision for a fractal dimension of the front.

Main equations of the convective hydrodynamic model

Many authors (e.g. Iben, 1982) use the hydrostatic system of equations with adiabatic convection in the stellar core, when calculating the presupernova evolution (with time-scale $\sim 10^4 \text{ yr}$) which is valid for this stage, but is too crude at the beginning of the thermal runaway. We carried our calculations both on the presupernova stage and on the stage of explosive burning by the hydrodynamic scheme elaborated in papers by Blinnikov and Rudzsky (1984), Blinnikov and Bartunov (1993), and by Blinnikov and Dunina-Barkovskaya (1993, 1994). In the latter two papers this hydrodynamic scheme was used for the calculation of white dwarf evolution. Here we have included non-adiabatic time-dependent convection in well-known mixing length approximation:

$$\partial r / \partial t = v, \quad (2)$$

$$\partial v / \partial t = -Gm/r^2 - 4\pi r^2 (\partial P / \partial m), \quad (3)$$

$$\partial T / \partial t = [\varepsilon_{CC} + \varepsilon_\nu + \varepsilon_g - 4\pi \partial(r^2 F_{\text{conv}}) / \partial m$$

$$- 4\pi \partial(r^2 F_{\text{rad}}) / \partial m] / (\partial E / \partial T)_\rho, \quad (4)$$

$$\partial X_C / \partial t = -X_C^2 r_{CC} + (\partial X_C / \partial t)_{\text{conv}}, \quad (5)$$

$$\partial u_c / \partial t = 2(v_c^2 - u_c^2) / l_{\text{mix}}, \quad (6)$$

where X_C is the mass fraction of ^{12}C , ε_{CC} is the energy release during the carbon burning, ε_ν stands for standard neutrino energy losses (as approximated by Schinder et al., 1987; see also Haft et al., 1994), ε_g is the energy liberation during the gravitational contraction, F_{rad} is the radiative energy flux, F_{conv} is the convective energy flux, u_c is the time-dependent convective velocity (see Arnett 1969), and v_c is the stationary convective velocity in the mixing length approximation which is given by the formula (see, e.g., Bisnovatyi-Kogan, 1989)

$$v_c = (g(\partial \ln \rho / \partial r - (\partial \ln \rho / \partial r)_S))^{1/2} \cdot l_{\text{mix}} / 2. \quad (7)$$

The convective energy flux F_{conv} and the value $(\partial X_C / \partial t)_{\text{conv}}$, which corresponds to the change of a carbon mass fraction X_C by convection, were calculated by the formulas

$$F_{\text{conv}} = ((\partial T / \partial r)_S - \partial T / \partial r) c_p \rho u_c l_{\text{mix}} / 2, \quad (8)$$

$$\left(\frac{\partial X_C}{\partial t} \right)_{\text{conv}} = \frac{1}{r^2} \frac{\partial}{\partial r} \left(r^2 l_{\text{mix}} u_c \frac{\partial X_C}{\partial r} \right). \quad (9)$$

The arrangement and the sizes of the convective zones are defined by the Schwarzschild criterion (according to the aforesaid formulas (7) and (8)). On the presupernova stage we did not account for time-dependent convection and the formulas (8–9) contained v_c instead of u_c . A comparison of calculations with stationary and time-dependent convection on the supernova stage was performed in (Dunina-Barkovskaya, Imshennik, 2000).

The mixing length in the i -th mass zone was determined by the relation

$$l_{\text{mix}}^{(i)} = \min(\alpha_P (\partial |\ln P| / \partial r)_i^{-1}, \alpha_c \Delta r_c), \quad (10)$$

where Δr_c is the size of the convective zone containing i -th zone, and α_P in our calculations was taken equal to unity.

Thermodynamic functions for the electron-positron gas (the pressure P , the entropy S etc.) were calculated with help of Nadyozhin's asymptotic realtions described by Blinnikov et al. (1996), and for the ionic gas with screening — by Yakovlev and Shalybkov (1988).

Initial and boundary conditions. Computations on the presupernova stage

The initial state of the presupernova C–O core should to be taken from reliable evolutionary calculations. We begin our computations with the central density 10^9g cm^{-3} which, according to Iben (1982), corresponds to the central temperature about $T_c^{(0)} = 2.05 \cdot 10^8 \text{K}$. Everywhere below we define, as a beginning of the runaway and, thereafter, as an end of the presupernova stage, the moment of time when the temperature in the central zone reaches the value of $5 \cdot 10^9 \text{K}$.

The initial carbon mass fraction $X_C^{(0)} = 0.27$ (constant throughout the C–O core) was taken the same as in Iben's (1982) work. Assuming the above-mentioned central parameters for the C–O core and its total mass $1.33M_\odot$, we have computed the adiabatic configuration in hydrostatic equilibrium which was used as an initial condition. It should be mentioned that its difference from Iben's (1982) model seems insignificant.

During the calculations of the evolution of this model with account for a constant mass growth-rate $5 \cdot 10^{-7} M_\odot \text{yr}^{-1}$ (typical for accreting white dwarfs in binary systems), it is worth-while to set a non-zero outer boundary condition for the pressure. In our previous work (Dunina-Barkovskaya, Imshennik, 2000), where the calculations led to relatively small changes of the total mass before the runaway, we included all the accreting mass in the outer boundary condition.

This condition is easily derived in the approximation of a thin ($\Delta R/R \ll 1$) and light ($\Delta M/M \ll 1$) envelope. Really, by integrating the hydrostatic equilibrium equation $-dP/dm = Gm/4\pi r^4$ over the en-

velope thickness we obtain for the pressure P_b on the outer boundary of the zone with the Lagrangean coordinate M :

$$\begin{aligned} P_b(M) &= \frac{G}{4\pi} \int_M^{M+\Delta M} \frac{m dm}{r^4} \simeq \frac{G}{8\pi R^4} (m^2)_M^{M+\Delta M} \\ &\simeq \frac{GM}{4\pi R^4} \Delta M, \end{aligned} \quad (11)$$

where $\Delta M = \dot{M}t$ and $R = R(t)$ during the hydrostatic evolution, i.e. the outer pressure P_b from (11) increases in proportion to the time t which is measured from the beginning of the C–O core evolution calculations.

In this case the full mass $M_N + \Delta M$ (where M_N is the mass of N Lagrangean zones contained in the hydrodynamic model) grew up to $\sim 1.351M_\odot$, in accordance with evolution time $4.25 \cdot 10^4 \text{yr}$ (Dunina-Barkovskaya, Imshennik, 2000).

In the present work, we have gradually, according to the accretion, added new Lagrangean zones to the model (cf. Woosley, 1997). The mass of the zones decreased geometrically from $7.83 \cdot 10^{-3} M_\odot$ (151-th zone) down to $7.50 \cdot 10^{-5} M_\odot$ (the last, 170-th zone). It was found in this case that the equation (11) is quite inaccurate (evidently because $\Delta R/R$ is not very small). As a result, the evolution time on the presupernova stage increased nearly twice. For the variants with non-zero α_c the mass of the model reached $1.3658M_\odot$ after $t \simeq 7.2 \cdot 10^4 \text{yr}$, and the number of the Lagrangean zones became $N = 170$. After that we have added no Lagrangean zones, but simulated accretion by increasing the outer pressure. In the runaway point (after $t \simeq 7.9 \cdot 10^4 \text{yr}$ since the beginning of calculations) the outer pressure corresponded to the additional external mass from $2.316 \cdot 10^{-3} M_\odot$ (for $\alpha_c = 3.0 \cdot 10^{-4}$) to $2.342 \cdot 10^{-3} M_\odot$ (for $\alpha_c = 4.0 \cdot 10^{-3}$). In the control variant with $\alpha_c = 0$ the temperature in the central zone increased to $5 \cdot 10^9 \text{K}$ already after $6.789 \cdot 10^4 \text{years}$, therefore the model mass could grow only up to $1.3636M_\odot$, which corresponds to the number of zones $N = 161$.

Let us consider the boundary condition (11) during the explosion for the variant with $\alpha_c = 1.0 \cdot 10^{-3}$ when $\Delta M = 2.338 \cdot 10^{-3} M_\odot$, and $R_0 = 1.85 \cdot 10^8 \text{cm}$

(Fig. 1):

$$P_b(1.33M_\odot) = P_0 \left(\frac{R_0}{R} \right)^4. \quad (12)$$

where $P_0 = 5.72 \cdot 10^{22} \text{din cm}^{-2}$. This value is to be compared with the central pressure of the C–O core which has the well-known lower estimate $P_c(0) > GM^2/(8\pi R^4)$. Thus, the ratio of the outer boundary pressure to the central one, $P_b(M)/P_c(0) < 2\Delta M/M = 3.42 \cdot 10^{-3}$, is surely very small at the beginning of the runaway. In the subsequent runaway process it certainly changes and can increase by factor of a few, but nevertheless remains small enough which can be seen from the numerical results.

It is easy to estimate that the relative contribution of the inertial term into the derived boundary condition (12) with characteristic parameters of C–O core pulsations $(4v_p/\tau_p) \cdot (R_0^2/(GM))$ will be small: no more than a few percent. Thus we can neglect it in (11) even when the pulsations amplitude is maximal $\Delta R \simeq R_0$ and $\tau_p \simeq 5\text{c}$ by the end of deflagration burning (See Fig. 4). This boundary condition imposed by the mass accretion onto the C–O core surface is in close agreement with the outer boundary condition assumed in the previous works (Ivanova et al., 1974; Ivanova et al., 1977a) with the same dependence on an outer radius R : $P_b(M) \propto R^{-4}$ (12). Let us remind that in the cited works the outer pressure also simulated the presence of the outer C–O core envelope. It was taken small enough, but about a factor of 2 higher than the value from (12). Thus, the effect of the outer boundary was more pronounced there than in the present work, but less significant than in (Dunina-Barkovskaya, Imshennik, 2000). It should be stressed that the non-zero outer pressure $P_b(M) \neq 0$ violates the energy conservation law during the explosion (see Fig. 4, 5) when the pulsations arise and the radius R of the C–O core changes. Naturally, accounting for the accreting matter in the outer boundary condition (11) and (12) we imply its attachment to the evolving C–O core without any further energy release, i.e. merely an adhesion. In fact, this substance has, generally speaking, another chemical composition, and can go through the thermonuclear reactions with an energy liberation and even

with partial ejection of the accreted material. We simply neglect those processes. On the other hand, the role of the outer boundary condition (12) is very significant during the explosion, especially when the detonation wave forms near the surface (see below).

The discussion of the results

In the present work we have systematically investigated the models numerically with different values of the mixing length parameter (10) equal to $\alpha_c = 4.0 \cdot 10^{-3}$; $3.0 \cdot 10^{-3}$; $2.0 \cdot 10^{-3}$; $1.0 \cdot 10^{-3}$; $3.0 \cdot 10^{-4}$. From a physical standpoint, it is very difficult to choose a certain value α_c from this wide range in the used approximate theory of non-adiabatic convection. The energy release in the thermonuclear reaction of carbon burning $^{12}\text{C}+^{12}\text{C} \rightarrow ^{24}\text{Mg}+\gamma$ was taken, first, by a rather crude formula obtained by Fowler and Hoyle (1965) with electron screening factor by Salpeter (1954) (see also Salpeter and Van Horn 1969, and Arnett 1969), and, second, with a maximum possible energy liberation corresponding to the instantaneous combustion of all the carbon-oxygen mixture to ^{56}Ni . The energy release accepted here was taken from our early work (Ivanova et al. 1974). It is convenient for the further comparison of our previous results with those obtained in the current work. Such a simplification of a thermonuclear energy generation cannot affect essentially the obtained results due to the comparatively small sensitivity of the ignition conditions for the C–O mixture to all pre-exponential values in the expression for the thermonuclear burning rate.

As a result of the presupernova evolution calculations we obtained that just prior to the runaway the density drops to a value which depends non-monotonically on the parameter α_c and is maximal when $\alpha_c = 4.0 \cdot 10^{-3}$. In general, the initial critical central density (in units 10^9g cm^{-3}) $\rho_{c \text{ cr } 9} \simeq (1.88 - 2.03)$ turned out to be close to the one accepted earlier by Ivanova et al. (1974) and later by Ivanova et al. (1977a) ($\rho_{c9} = 2.33$), though it is somewhat lower. Let us remind that in 1970s the most popular viewpoint was that single intermediate mass stars evolve along the convergent Paczyński's (1970) track

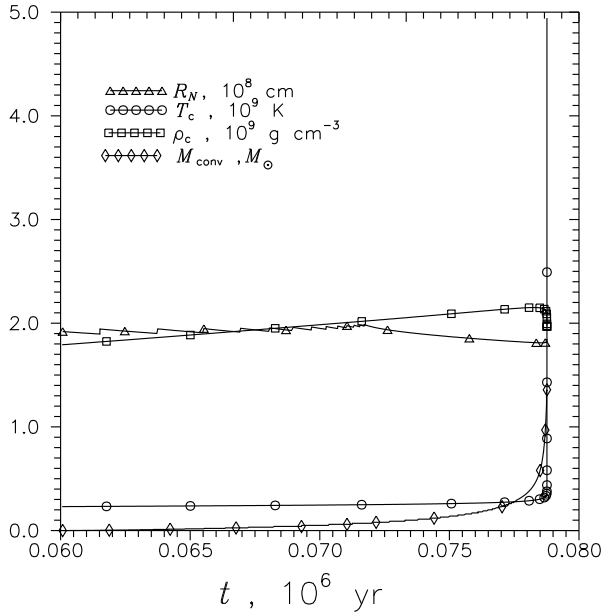


Figure 1: The presupernova evolution: the dependence of the central temperature T_c , the central density ρ_c , the convective core mass M_{conv} , and the radius R_N of the N -th (last) Lagrangean zone upon time for $\alpha_c = 1.0 \cdot 10^{-3}$ after the convective core formation.

after the formation of the carbon (or carbon-oxygen) core. The modern approach to the presupernova evolution involves the evolution in a close binary system with an accreting white dwarf. In this case, according to Yungelson (1998), all the stars in the initial main sequence mass range $2.5 \leq M/M_\odot \leq 10$ may become carbon-oxygen white dwarfs in close binary systems. This range does not differ significantly from the similar range for single stars $3.5 \leq M/M_\odot \leq 8$ considered previously (Paczynski, 1970).

Some quantities characterizing the C–O stellar core before the runaway are represented in Fig. 1: the convective core mass M_{conv} , the central temperature T_c , the central density ρ_c , and the radius of the C–O core R_N over the evolution time from $6 \cdot 10^4$ yr (the beginning of the convective core formation) to $7.87 \cdot 10^4$ yr for $\alpha_c = 1.0 \cdot 10^{-3}$. Small jumps in the radius of the last (N -th) Lagrangean zone shown on Fig. 2

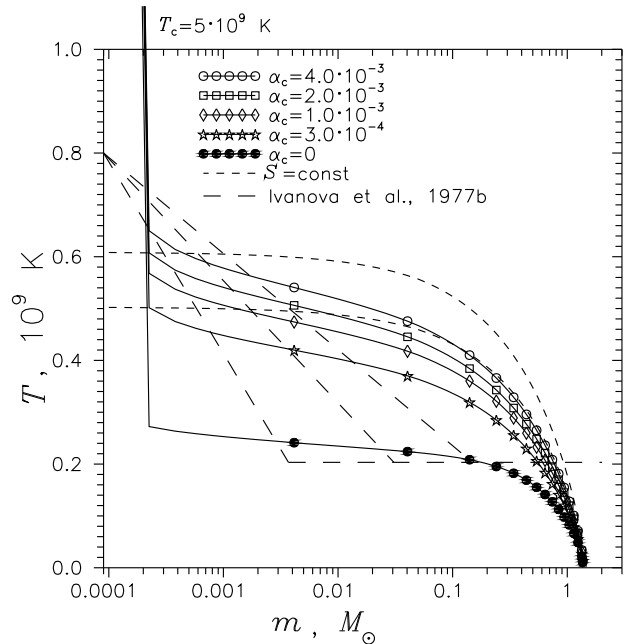


Figure 2: The temperature profiles at the beginning of the SN stage (when the central temperature reaches $5 \cdot 10^9$ K) for various values of the parameter α_c .

clearly indicate the procedure of adding of new Lagrangean zones described above. The phase of the slow expansion before the runaway (see above) is almost unnoticeable on this graph because its duration ($\sim 3 \cdot 10^2$ yr) is small in comparison to the overall evolution time (during which the star, as a whole, was contracting very slowly) and practically does not depend on α_c .

In Fig. 2, the initial profiles of temperature depending on the mass coordinate are represented at the moment of the beginning of explosion (see above). It can be seen that the temperature in the convective variants is appreciably higher than that in the variant without convection. Even for $\alpha_c = 3.0 \cdot 10^{-4}$ the temperature exceeds this value almost by a factor of 2 in the central part of the convective core. Let us notice that in this moment there is an active combustion only in the first mass zone. On Fig. 2 we compare the initial temperature profiles with data from

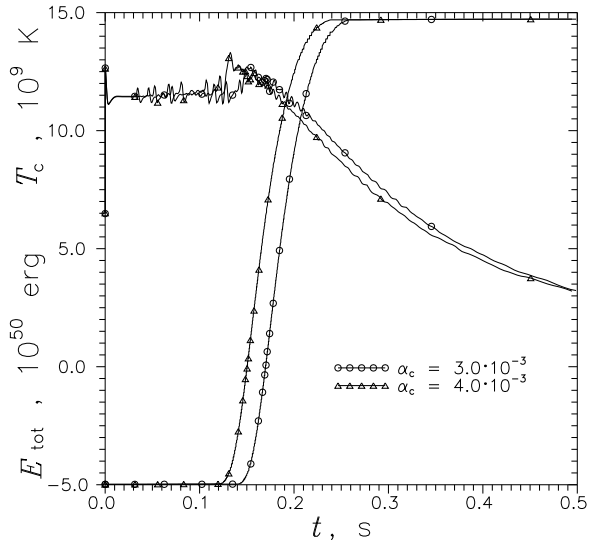


Figure 3: The time dependence of the central temperature T_c and of the full energy of the C–O core E_{tot} for $\alpha_c = 4.0 \cdot 10^{-3}$ and $3.0 \cdot 10^{-3}$ (prompt detonation).

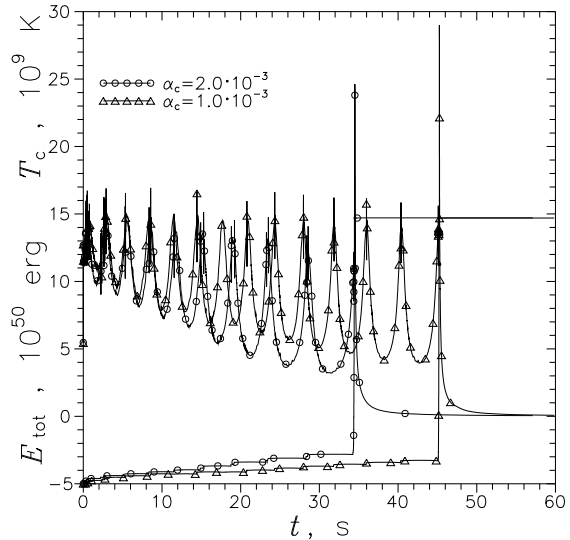


Figure 4: The time dependence of the central temperature T_c and of the full energy of the C–O core E_{tot} for $\alpha_c = 2.0 \cdot 10^{-3}$ and $\alpha_c = 1.0 \cdot 10^{-3}$ (pulsational deflagration with delayed detonation).

Ivanova et al. (1977b). In the latter work the explosion developed for the two (upper) T -profiles. Therefore, it is not surprising that the runaway led to the total disruption of the star for all $\alpha_c \geq 3.0 \cdot 10^{-4}$ in the present calculation (see below). For the variants with $\alpha_c = 2.0 \cdot 10^{-3}$ and with $\alpha_c = 3.0 \cdot 10^{-4}$ which are the boundary values for the deflagration regime with pulsations (see below), the adiabatic temperature profiles are also shown, with the entropy equal to the entropy of the 2nd mass zone for each variant. It can be seen that our profiles lie quite below the corresponding adiabatic profiles, and they have another shape for $m < 0.1M_\odot$, which of course can affect the development of the runaway without the regime of spontaneous burning (Blinnikov, Khokhlov, 1986).

It is interesting that in the second mass zone (with $m = 2.24 \cdot 10^{-4}M_\odot$) the smooth temperature profile for the maximum $\alpha_c = 4.0 \cdot 10^{-3}$ touches the third (lower) steep profile for which the explosion in (Ivanova et al., 1977b) failed. But the initial profile for the variant with the minimal $\alpha_c = 3.0 \cdot 10^{-4}$ which in fact "hardly" exploded (see Fig. 5) already lies noticeably below the third profile from (Ivanova

et al., 1977b) for $m < 7 \cdot 10^{-4}M_\odot$ (in the first 4 mass zones). We can conclude that there is a qualitative agreement between our present results and the calculations in the cited work.

The development of the runaway was different for $\alpha_c \geq 3.0 \cdot 10^{-3}$ (Fig. 3) and for $\alpha_c \leq 2.0 \cdot 10^{-3}$ (Fig. 4). On the said graphs the time dependence of the central temperature T_c and of the full energy of the C–O core E_{tot} on time is shown. The latter eventually becomes equal to the value $\sim 1.5 \cdot 10^{51}$ erg corresponding to the full incineration into ^{56}Ni for all the variants regardless of the value α_c . The value of E_{tot} at the moment of the runaway beginning ($-4.3 \cdot 10^{50}$ erg) is also practically the same for all this variants.

The basic result of our numerical calculations is that the pulsational deflagration regime eventuates when the mixing length is small enough, namely $\alpha_c \leq 2.0 \cdot 10^{-3}$. It was found that for $\alpha_c \geq 3.0 \cdot 10^{-3}$ the prompt detonation occurs (see Fig. 3). Hereby we obtained a reasonably accurate threshold for the transition from the detonation to the pulsational deflagration.

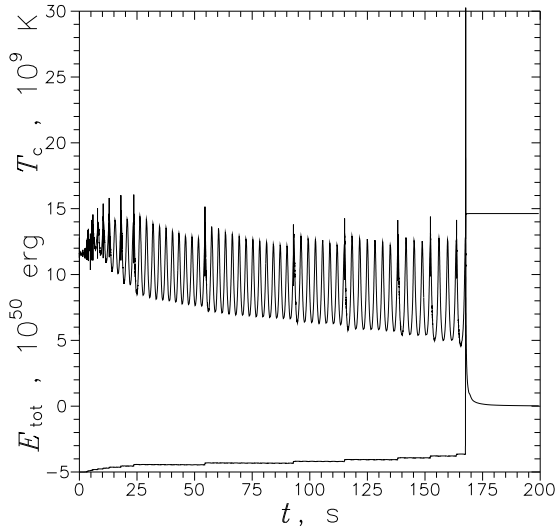


Figure 5: The time dependence of the central temperature T_c and of the full energy of the C–O core E_{tot} for $\alpha_c = 3.0 \cdot 10^{-4}$ (pulsational deflagration with delayed detonation).

On Fig. 4 there is 10 pulsations for the variant with $\alpha_c = 2.0 \cdot 10^{-3}$ and 14 pulsations for the variant with $\alpha_c = 1.0 \cdot 10^{-3}$. In both cases the burning ends with a powerful energy release in the last pulsation. In this case the abrupt change of the burning regime occurs. In the previous pulsations there was a deflagration regime, and in the last pulsation the all remaining fuel (about 90%) is burning in the regime of detonation. The value T_c reaches its maximal value $(2.5 - 2.9) \cdot 10^{10}$ K a bit later, immediately after the collision of the detonation front propagating inward from the surface and deflagration front, during the afterburning in the central zone). Thus, the hybrid regime of the thermonuclear explosion of a carbon-oxygen white dwarf takes place, which is most promising for the explosive nucleosynthesis (Niemeyer and Woosley, 1997). On the other hand, Fig. 3 demonstrates the burning without pulsations in an ordinary detonation regime starting from the center (for $\alpha_c \geq 3.0 \cdot 10^{-3}$).

In Fig. 5, the time dependence of the central temperature and of the total energy is shown for the com-

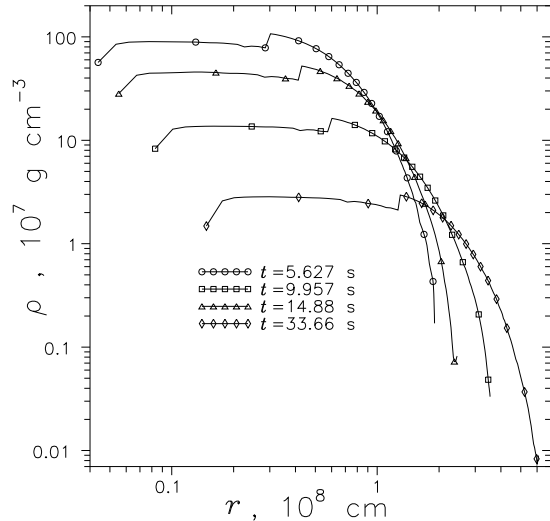


Figure 6: The density profiles versus radius for $\alpha_c = 1.0 \cdot 10^{-3}$ (pulsational deflagration).

putation with $\alpha_c = 3.0 \cdot 10^{-4}$. Here the total number of pulsations is appreciably larger than on the previous graph, but only 14 of them were accompanied by the propagation of deflagration into a neighboring mass zone, which can be well seen by very narrow specific maxima of the temperature T_c . Let us notice that these narrow maxima correspond (due to the energy generation) to the small jumps of the value E_{tot} . In the variant with $\alpha_c = 1.0 \cdot 10^{-3}$ one to three mass zones were burning during each pulsation (except for 5th and 7th), so almost all the pulsations had the said temperature peaks (Fig. 4).

The deflagration regime is distinctly characterized by the profiles of density which are represented versus the Eulerian radius r in Fig. 6 for $\alpha_c = 1.0 \cdot 10^{-3}$. The density drops by a factor of 1.5 at the deflagration front. Depending upon the pulsation phase the front either moves inward (the contraction phase) or outward (the expansion phase) during the overall propagation (by mass zones). The pulsations can be seen more clearly by the behaviour of the outer layers of the star, in the still unburnt matter. The amplitude of the outer radius pulsations grows in time and attains the value of ~ 1.5 (this can be seen well due to the logarithmic scale for density in Fig. 6).

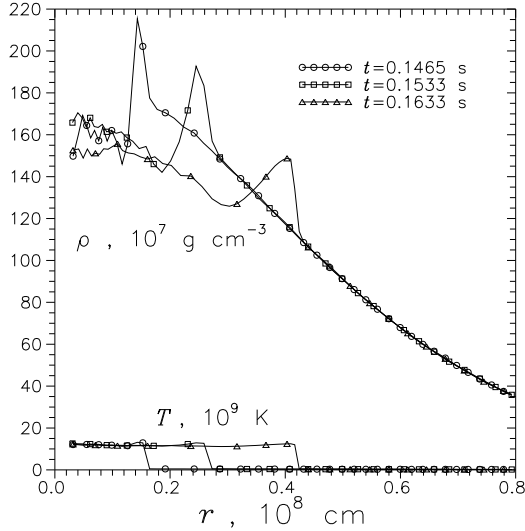


Figure 7: The density and temperature profiles versus radius for $\alpha_c = 3.0 \cdot 10^{-3}$ (prompt detonation).

The density profiles $\rho(r)$ for stronger convection are given in Fig. 7 for $\alpha_c = 3.0 \cdot 10^{-3}$. The profiles of the temperature $T(r)$ are plotted on this graph in a small scale, they show neatly the position of the burning front as a jump of T . It can be seen that at the burning front the density of matter distinctly increases displaying the detonation burning regime. The supersonic character of detonation is also revealed by the quiescence of stellar layers outside the burning front.

The convective processes are most neatly characterized by the profiles of the specific entropy which are shown in Fig. 8 for the case $\alpha_c = 1.0 \cdot 10^{-3}$ versus the mass coordinate m (in logarithmic scale). The convective zones which are defined by the known Schwarzschild criterion, i.e. correspond to the regions with the negative entropy gradient, are marked on these profiles for some typical moments of time. This figure shows that the primary convective core during the runaway is being separated into some convective zones, the largest of which includes one of two mass zones behind the burning front and the rest of the convective core before the front. The separation process is of nonstationary character and indicates the

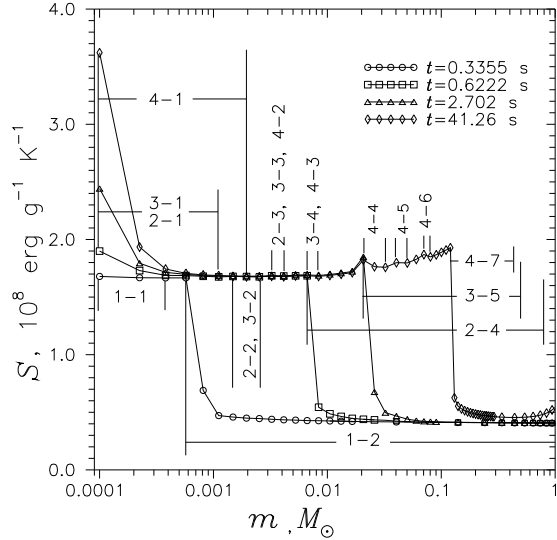


Figure 8: The entropy profiles versus mass for $\alpha_c = 1.0 \cdot 10^{-3}$ (before the detonation). Convective zones are shown by labels and numbers, e.g. 2-1 means the first convective zone for the second moment ($t=0.6222$ s).

importance of the time-dependent convection.

The entropy profiles are given in Fig. 8 before the formation of the detonation wave propagating towards the center (see Fig. 4). After the formation inception of such a wave, naturally, in a very short time ~ 0.1 s, the entropy behind the detonation front rises to the values which are typical also for the deflagration, $(2-3) \cdot 10^8 \text{erg g}^{-1} \text{K}^{-1}$, i.e. by factor of 4-6 more than an initial entropy ($\sim 0.5 \cdot 10^8 \text{erg g}^{-1} \text{K}^{-1}$), with a positive gradient. Only in outer layers (with $m \gtrsim 1.36 M_\odot$) the negative entropy gradient persists, and, therefore, the convection occurs, partly preventing the detonation process described here.

The important role of the convection intensity characterized by a parameter α_c attracts our special attention. It is clear that the deflagration burning regime with pulsations (of course, the deflagration is not necessarily accompanied by pulsations, but for the latter the subsonic deflagration is the necessary condition) takes place in the whole range of the α_c values, $\alpha_{c \text{ min}} \lesssim \alpha_c \lesssim 2.0 \cdot 10^{-3}$. It is essential that

$\alpha_{c \text{ min}}$ is above zero, because for $\alpha_c = 0$ in our calculation there was no hydrodynamic explosion at all, although the first mass zone was burning. We note that for higher critical densities $\rho_{c \text{ cr}}$ which is the case for lower accretion rate (see above), the value of $\alpha_{c \text{ min}}$ can drop practically down to zero (Zmitrenko et al., 1978). However, for high densities $\rho_{c \text{ cr}}$ the account for neutrino energy losses together with the neutronization kinetics is required (Ivanova et al., 1977a,c). But in the present case ($\rho_{c \text{ cr}} \simeq 2 \cdot 10^9 \text{ g cm}^{-3}$) the role of these complicated processes is not important, which was shown by direct comparison of the calculations of Ivanova et al. (1974) with those of Ivanova et al. (1977b) at the close value of central density $\rho_c = 2.33 \cdot 10^9 \text{ g cm}^{-3}$. Thus, the account for convection processes can prevent the pulsations development during the deflagration burning when the parameter α_c exceed some critical value $\alpha_{c \text{ crit}}$. In the present work it is found that $\alpha_{c \text{ crit}} \gtrsim 3.0 \cdot 10^{-3}$.

A qualitative analysis of the physical conditions of the delayed detonation

In essence, the emergence of the detonation, after a long period of the deflagration burning accompanied by the development of the global pulsations of the C–O core, can be termed a "delayed detonation" (Niemeyer and Woosley, 1997): from the moment of the central ignition a long time (tens of seconds) passes, i.e. many thermodynamic time-scales of the order of the pulsation period, 2–3 s. An analysis of the results has shown that the detonation burning front emerges in a mass coordinate about $1.33M_\odot$, more specifically, in the 150th mass zone when the total number of zones equals 170. This coordinate is virtually independent of the parameter α_c . In our model in the 150th zone the mass grid changed from uniform to geometrically decreasing. In the work (Dunina-Barkovskaya, Imshennik, 2000) the 127th mass zone in which the detonation begins had the same feature, so we have to investigate the influence of a mass grid nonuniformity on a detonation initiation in our future work. In the present section we shall try to give

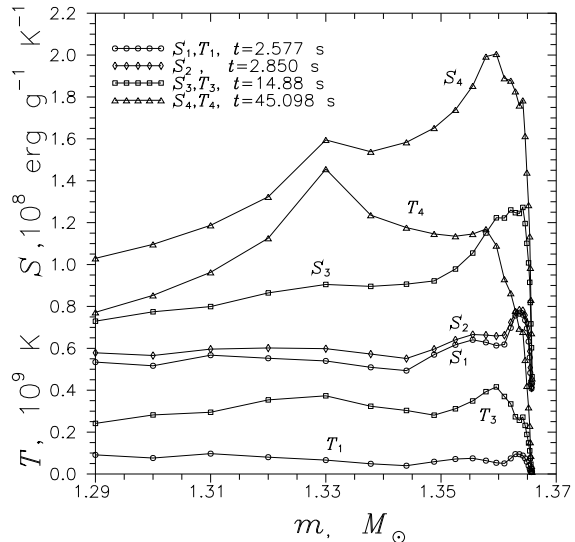


Figure 9: The entropy profiles versus mass in the outer layers of the C–O core for $\alpha_c = 1.0 \cdot 10^{-3}$ during the delayed detonation (up to the beginning of last pulsation with the detonation initiation).

a physical justification of the entropy growth that leads to the detonation.

After some first pulsations, i.e. long before the generation of the burning front, the entropy of the outer mass zones begins to increase (Fig. 9). At the moment $t = 45.098$ s (the beginning of the last pulsation) two local entropy maximums exist, the outermost one ($m \simeq 1.36M_\odot$) and the innermost one ($m \simeq 1.33M_\odot$). Though the entropy in the innermost maximum is less than in the outermost one, the temperature in the innermost maximum during the last pulsation is higher (due to the higher density). Just at this maximum the detonation burning front is born (see Fig. 11). We can see the relatively high growth of entropy between the close moments $t = 2.577$ s and $t = 2.850$ s, between the maximum and the minimum of the second (!) pulsation (see Fig. 4), which is less by amplitude than the subsequent pulsations.

It can be seen on the graphs for density (Fig. 10) that the moments close to the maxima of pulsations are accompanied by a subsequent emergence of the

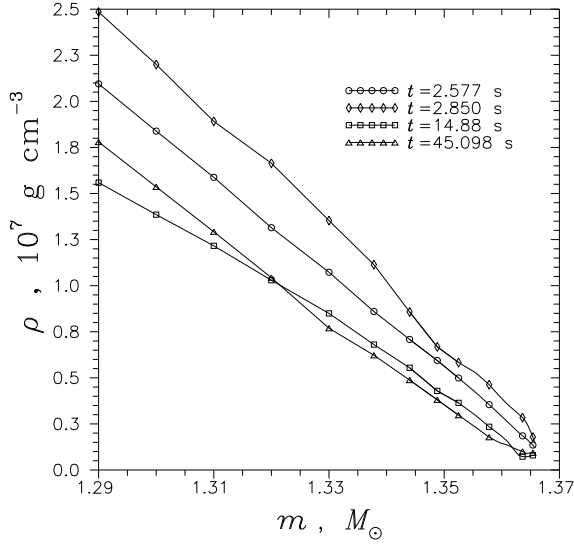


Figure 10: The density profiles versus mass in the outer layers of the C–O core for $\alpha_c = 1.0 \cdot 10^{-3}$ (pulsational deflagration up to the detonation initiation).

compression waves on the stellar surface. Following Ivanova et al. (1982), one can estimate the entropy growth ΔS treating these compression waves as weak shocks with a pressure jump ΔP . The one gets the well-known entropy jump (Landau and Lifshitz, 1954):

$$\Delta S = \frac{1}{12T_1} \left(\frac{\partial^2 V}{\partial P_1^2} \right)_S (\Delta P)^3. \quad (13)$$

This estimate is easy to apply in the case under consideration because we can account only for the pressure of the completely degenerate ultrarelativistic electron gas $P_{1e} = K\rho_1^{4/3}$, with $K = 4.90 \cdot 10^{14} \text{cm}^3 \text{g}^{-1/3} \text{s}^{-2}$, in calculation of the second adiabatic derivative in (13), whence it follows that

$$\left(\frac{\partial^2 V}{\partial P_1^2} \right)_S = \left(\frac{\partial^2 V}{\partial P_1^2} \right)_{S=0} = \frac{d^2 V}{dP_{1e}^2} = \frac{21}{16} \frac{1}{K^2 \rho_1^{11/3}}. \quad (14)$$

Such an approximation is possible because in the zone under consideration with $m = 1.33M_\odot$ we can take as an estimate for the values ρ_1 and T_1 in front of the involved weak shock their values at the moment $t = 2.577$ s, namely, $\rho_1 = 1.073 \cdot 10^7 \text{g cm}^{-3}$, and

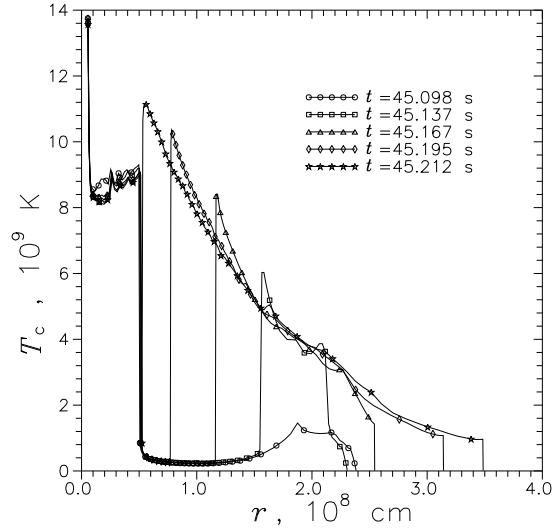


Figure 11: The temperature profiles versus radius during the delayed detonation for $\alpha_c = 1.0 \cdot 10^{-3}$.

$T_1 = 6.64 \cdot 10^7 \text{K}$. After a simple rearrangement we get the final expression for the specific entropy growth in (13) (S is in units $10^8 \text{erg g}^{-1} \text{K}^{-1}$, see Fig. 9):

$$\begin{aligned} \Delta S_8 &= 0.536 \cdot 10^6 \frac{\rho_1^{1/3}}{T_1} \left(\frac{P_2}{P_1} - 1 \right)^3 \\ &= 1.78 \left[\left(\frac{\rho_2}{\rho_1} \right)^{4/3} - 1 \right]^3. \end{aligned} \quad (15)$$

In the expression (15) it is necessary to specify also the amplitude of the weak shock wave. From Fig. 10 we can get $\rho_2 = 1.35 \cdot 10^7 \text{g cm}^{-3}$ (for the moment $t = 2.850$ s). Then we finally get from (15): $\Delta S_8 \simeq 0.085$, whereas in Fig. 9 the entropy growth between these two moments is $\Delta S_8 \simeq 0.06$. Thereby we can reasonably explain the entropy growth obtained in calculations as a result of a weak shock dissipation which occurs in the region of a rather abrupt density decrease. Closer to the surface the entropy growth subsides, according to (15), because of the density lowering towards the star edge, and inward it subsides too, probably due to the wave amplitude reduction (see also Fig. 10). Nevertheless, the local entropy maximum (Fig. 9) does not disappear with

time, but persists and increases furthermore by a factor of ~ 2.7 before the moment of the detonation generation. It reaches the value of $1.6 \cdot 10^8 \text{erg g}^{-1} \text{K}^{-1}$. Let us notice that unfortunately this cannot be seen on Fig. 8, because the outer stellar layer are shown there in the logarithmic scale by mass.

In Fig. 11, we represent the temperature profiles from the moment of the burning front initiation ($t = 45.098\text{s}$) to its "collision" with the deflagration front at a radius $r \simeq 5 \cdot 10^7 \text{cm}$ (which corresponds to the mass from the center $0.14M_\odot$) at the moment $t = 45.212 \text{s}$. On this graph the beginning of the expansion of matter behind the detonation wave can be well seen: the outer radius rises from $2.3 \cdot 10^8 \text{cm}$ to $3.5 \cdot 10^8 \text{cm}$ at the temperature $\sim 10^9 \text{K}$. When the detonation wave propagates in the direction of increasing density, the temperature rises to 10^{10}K , partly due to the heat capacity decline. The compression on the front is typically modest: only by a factor of 1.5 (see Fig. 7). The pressure jump is not high too: about a factor of 2 till the end. It is remarkable that the generation of the detonation front really occurs at the innermost entropy maximum (see Fig. 9), which corresponds in Fig. 11 to the innermost temperature maximum at the moment $t = 45.098 \text{s}$.

A fair question arises: whether such a detonation front is stable with respect to galloping instability considered recently by Imshennik et al. (1999). This question requires an additional analysis, but it is conceivable that the stability here is more natural, because the density in front of the detonation wave increases which counteracts the decoupling of the shock wave front from the burning zone. There is one more argument in favor of the stability against the multidimensional disturbances, namely, the large enough width of the burning zone which can be compared with the C–O core radius at the densities $\rho \sim 10^7 \text{g cm}^{-3}$ (Imshennik, Khokhlov, 1984). This implies also that the burning of the C–O mixture as a matter of fact does not fuse the elements to "iron" ("Fe") in the converging detonation wave, but is limited, for example, by such nuclides as Si etc. The problems of nucleosynthesis in the obtained regime of delayed detonation should be investigated in other works.

Conclusion

In the current study, first of all, we obtained the initial conditions, justified by evolution calculations, for the thermonuclear runaway in the carbon-oxygen stellar core with a mass close to the Chandrasekhar limit due to the accretion prescribed by a constant value $5 \cdot 10^{-7} M_\odot \text{yr}^{-1}$, which does not contradict to the current evolutionary studies of close binary systems. In our simulations the runaway begins at the moment defined by the calculation itself (and the equations do not change, except for the account for the time-dependent convection). Thus, we do not have to solve a complicated problem of the choice of the initial conditions, which largely affected the inception of the runaway. In our previous work (Ivanova et al., 1974, 1977a,b,c) the initial conditions (i. e. the initial temperature profiles) were defined, strictly speaking, without an adequate justification.

The present computations include a well-known approximate model of a nonadiabatic convection, namely, the mixing length theory with the only arbitrary parameter α_c (a ratio of the mixing length l_{mix} to the radial extent of the convective zone Δr_c). The value of this parameter could be, in principle, extracted from the multidimensional approaches developed currently (see Lisewski et al., 2000), i. e. the arbitrariness of the approximate theory could be removed. As a result of our computations it was found that the delayed detonation regime takes place under quite a wide range of values $3 \cdot 10^{-4} \lesssim \alpha_c \lesssim 2 \cdot 10^{-3}$. The lower boundary of this interval is defined as an upper estimate. At higher values of a parameter $\alpha_c \gtrsim 3 \cdot 10^{-3}$ in our calculations the ordinary detonation propagating from the center of the stellar C–O core was obtained, which is unlikely to take place because of the instability of the burning front etc. It could be interesting to find out whether the specified interval intersects with the region of effective mixing length parameters justified by a multidimensional theory of turbulence. But already with the parametric simulations of the flame propagation velocity we can impose some restrictions on the parameter α_c . For example, we can notice that for $\alpha_c = 1.0 \cdot 10^{-3}$ during the burning of a few first mass zones this velocity was close to the laminar front velocity obtained

by Woosley and Timmes (1992).

In the present work, due to an application of the new hydrodynamic code with a variable Lagrangean (difference) grid and with account for an outer boundary pressure conditioned by accretion, we have obtained a scenario of the development of a delayed detonation propagating from the surface towards the center of the star. The detonation is, in all probability, stable with respect to the galloping instability, and is conditioned by a preceding stage of the pulsational deflagration. This may prove to be important because of the recently emerged scepticism (Lisewski et al., 2000) in regard to the scenario of the deflagration to detonation transition due to the destruction of the laminar burning front by turbulent eddies published earlier (Khokhlov et al., 1997).

This work has been supported in part by the ISTC grant # 0370 and by the RFBR grant # 00-02-17230. The authors are grateful to W.Hillebrandt for the helpful discussion.

References

- Arnett W.D. // *Astrophys. Space Sci.*, 1969, v.5, p.180.
- Bisnovatyi-Kogan G.S. // *Physical problems of the theory of stellar evolution*. Moscow: Nauka, 1989.(in Russian)
- Blinnikov S.I., Bartunov O.S. // *Astron. Astrophys.*, 1993, v.273, p.106.
- Blinnikov S.I., Dunina-Barkovskaya N.V. // *Astronomy Reports*, 1993, v.37, p.187.
- Blinnikov S.I., Dunina-Barkovskaya N.V. // *MNRAS*, 1994, v.266, p.289.
- Blinnikov S.I., Dunina-Barkovskaya N.V., Nadyozhin D.K. // *Astrophys.J.Suppl.*, 1996, v.106, p.171.
- Blinnikov S.I., Khokhlov A.M. // *Sov.Astron.Lett.*, 1986, v.12, p.131.
- Blinnikov S.I., Rudzsky M.A. // *Sov.Astron.Lett.* 1984, v.10, p.152.
- Dunina-Barkovskaya N.V., Imshennik V.S. // *Proceedings of Lebedev Physical Institute*, 2000, v.227, p.32.
- Fowler W., Hoyle F. // *Nucleosynthesis in Massive Stars and Supernovae*. 1965. Chicago, University of Chicago Press.
- Hachisu I., Kato M., Nomoto K. // *Astrophys. J. Lett.*, 1996, v.470, L97.
- Haft M., Raffelt G., Weiss A. // *Astrophys.J.*, 1994, v.425, p.222.
- Iben I. // *Astrophys.J.*, 1982, v.253, p.248.
- Imshennik V.S., Kal'yanova N.L., Koldoba A.V., Chechetkin V.M. // *Astronomy Letters*, 1999, v.25, p.206.
- Imshennik V.S., Khokhlov A.M. // *Sov.Astron.Lett.*, 1984, v.10, p.262.
- Ivanova L.N., Imshennik V.S., Chechetkin V.M. // *Astrophys. Space Sci.*, 1974, v.31, p.497.
- Ivanova L.N., Imshennik V.S., Chechetkin V.M. // *Sov.Astron.*, 1977a, v.21, p.197.
- Ivanova L.N., Imshennik V.S., Chechetkin V.M. // *Sov.Astron.*, 1977b, v.21, p.374.
- Ivanova L.N., Imshennik V.S., Chechetkin V.M. // *Sov.Astron.*, 1977c, v.21, p.571.
- Ivanova L.N., Imshennik V.S., Chechetkin V.M. // *Sov.Astron.Lett.*, v.8, p.8.
- Khokhlov A.M., Oran E.S., Wheeler J.C. // *Astrophys.J.*, 1997, v.478, p.678.
- Landau L.D., Lifshits E.M. // *Mechanics of continua*. Moscow: Gos.izd-vo tekhniko-teor.lit.,1954. (in Russian)
- Lisewski A.M., Hillebrandt W., Woosley S.E. // *Astrophys.J.*, 2000, v.538, p.831.
- Niemeyer J.C., Woosley S.E. // *Astrophys.J.*, 1997, v.475, p.740.

- Nomoto K., Sugimoto D., Neo S. // *Astrophys. Space Sci.*, 1976, v.39, P.L37.
- Paczyński B. // *Acta Astronomica*, 1970, v.20, p.47.
- Salpeter E.E. // *Australian J.Phys.*, 1954, v.7, p.373.
- Salpeter E.E., Van Horn H.M. // *Astrophys.J.*, 1969, v.155, p.183.
- Schinder P.J., Schramm D.N., Wiita P.J., Margolis S.H., Tubbs, D.L.// *Astrophys.J.*, 1987, v.313, p.531.
- Woosley S.E. // *Astrophys.J.*, 1997, v.476, p.801.
- Woosley S.E., Timmes F.X. // *Astrophys.J.*, 1992, v.396, p.649.
- Yakovlev D.G., Shalybkov D.A. // *Itogi nauki i tekhn. ser. Astronomia*, 1988, v.38, p.191. (in Russian)
- Yungelson L.R. // *Contemporary problems of stellar evolution. Proceedings of the international conference in Zvenigorod. October 13–15 1998*, p.79.
- Zmitrenko N.V., Imshennik V.S., Khlopov M.Yu., Chechetkin V.M. // *Zhurn.Exp. i Teor.Fiz.*, 1978, v.48, p.589. (in Russian)